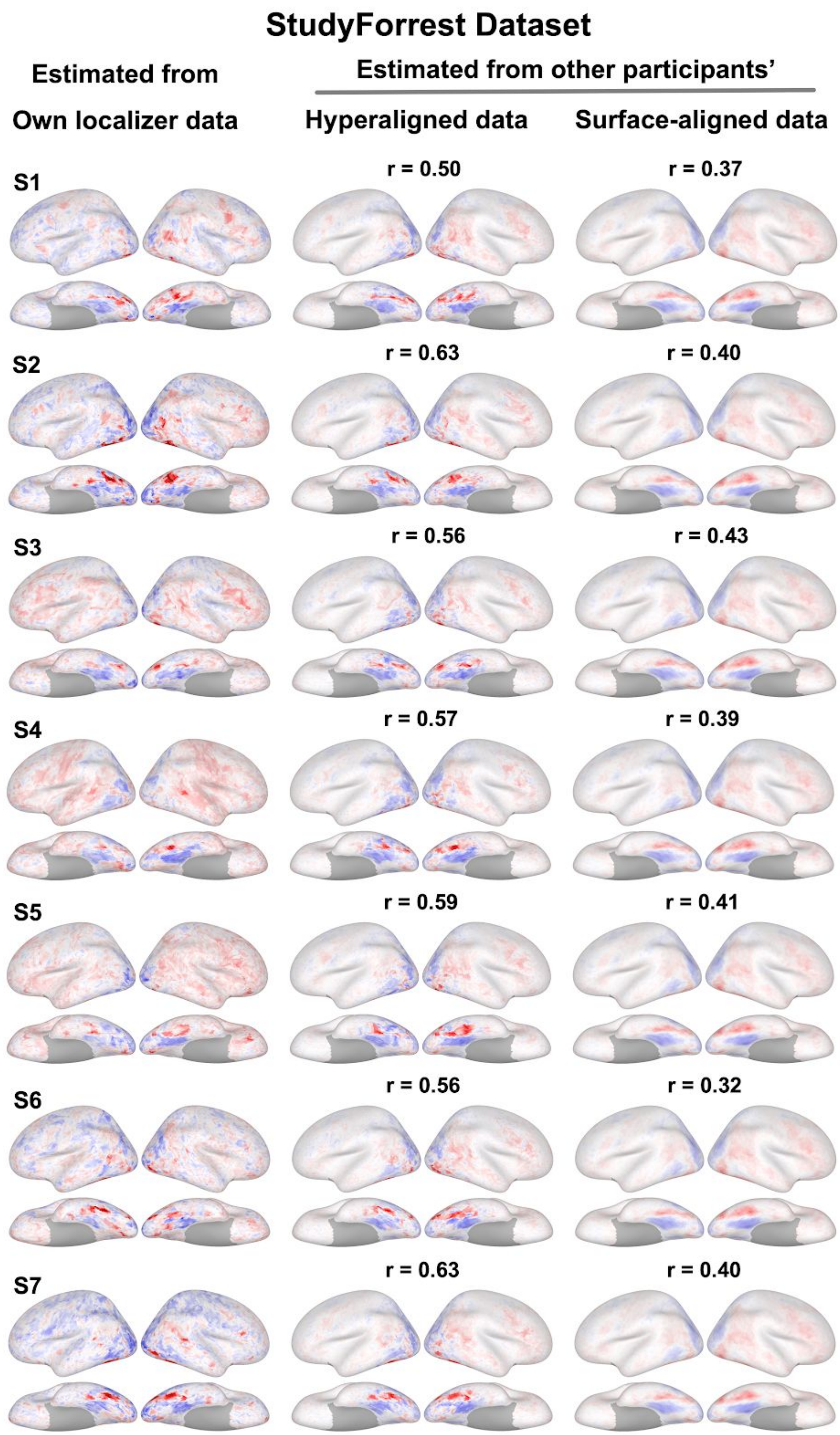
StudyForrest Dataset
Estimated from
Own localizer data
Estimated from other participants'
Hyperaligned data
Surface-aligned data
S1
r = 0.50
r = 0.37
S2
r = 0.63
r = 0.40
S3
r = 0.56
r = 0.43
S4
r = 0.57
r = 0.39
S5
r = 0.59
r = 0.41
S6
r = 0.56
r = 0.32
S7
r = 0.63
r = 0.40

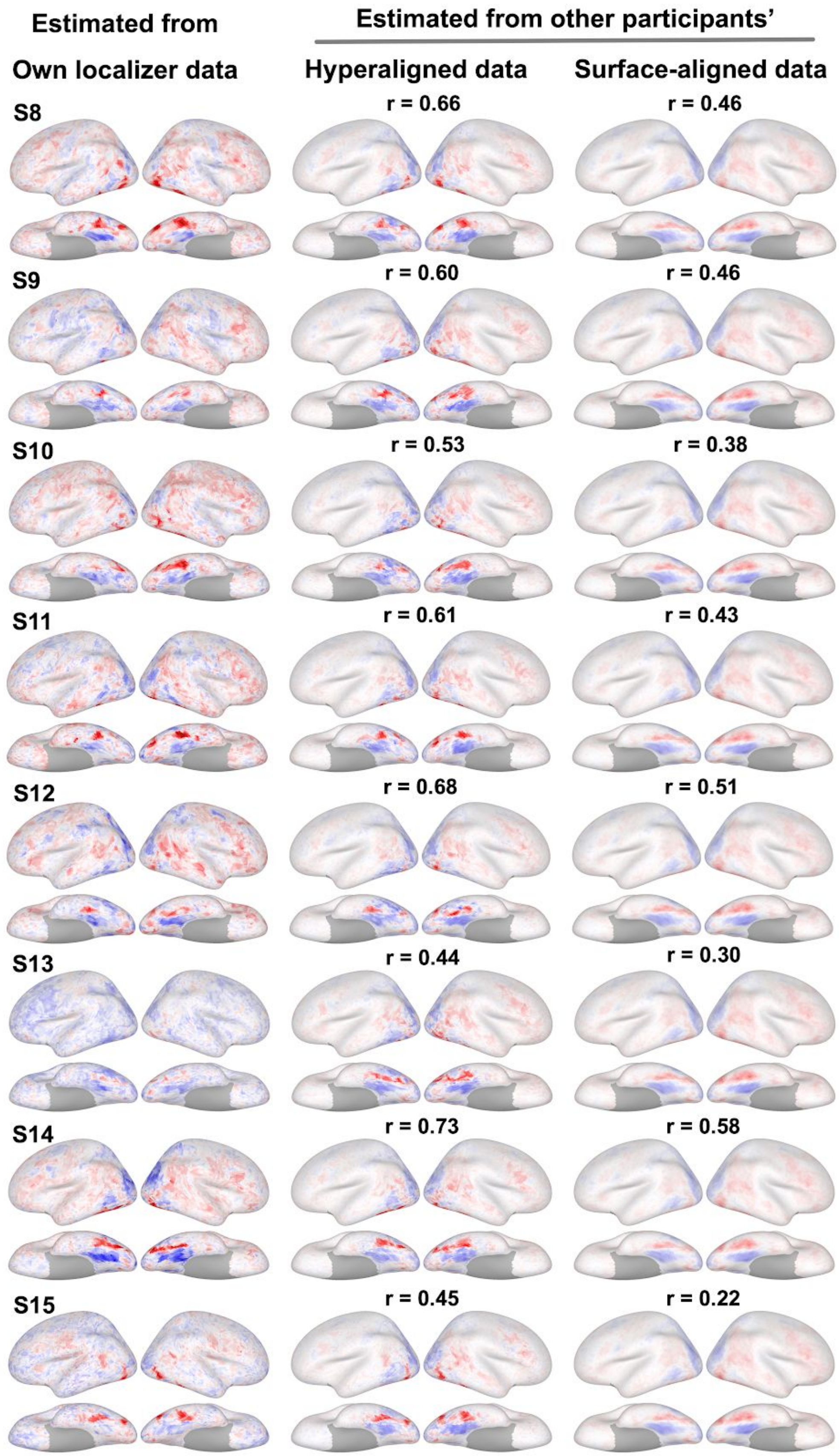
Estimated from
Estimated from other participants'
Own localizer data
Hyperaligned data
Surface-aligned data
S8
r = 0.66
r = 0.46
S9
r = 0.60
r = 0.46
S10
r = 0.53
r = 0.38
S11
r = 0.61
r = 0.43
S12
r = 0.68
r = 0.51
S13
r = 0.44
r = 0.30
S14
r = 0.73
r = 0.58
S15
r = 0.45
r = 0.22

**Supplementary Figure 1. Contrast maps of individual participant (StudyForrest dataset).** Contrast maps estimated from participants' own localizer data (face vs. all the other categories), the maps estimated from other participants' data with hyperalignment and with surface alignment were plotted for each participant in StudyForrest dataset. Correlation values above maps that were estimated from other participants' hyperaglined data indicate correlations between maps from participants' own data and the predicted maps with hyperalignment. Correlation values above maps that were estimated from other participants' surface-aligned data indicate correlations between maps from participants' own data and the predicted maps with surface alignment.

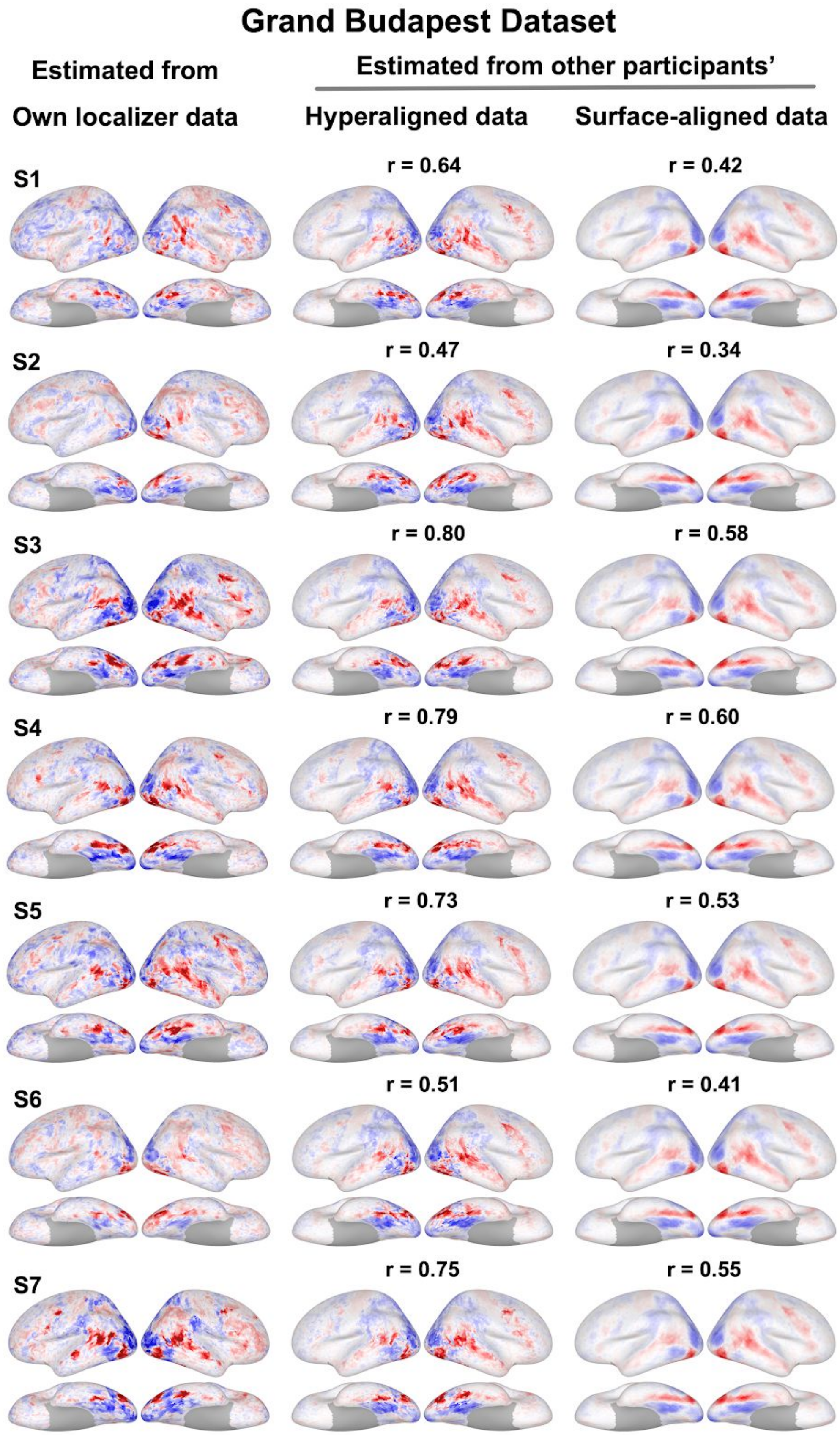
Grand Budapest Dataset
Estimated from
Own localizer data
Estimated from other participants'
Hyperaligned data
Surface-aligned data
S1
r = 0.64
r = 0.42
S2
r = 0.47
r = 0.34
S3
r = 0.80
r = 0.58
S4
r = 0.79
r = 0.60
S5
r = 0.73
r = 0.53
S6
r = 0.51
r = 0.41
S7
r = 0.75
r = 0.55

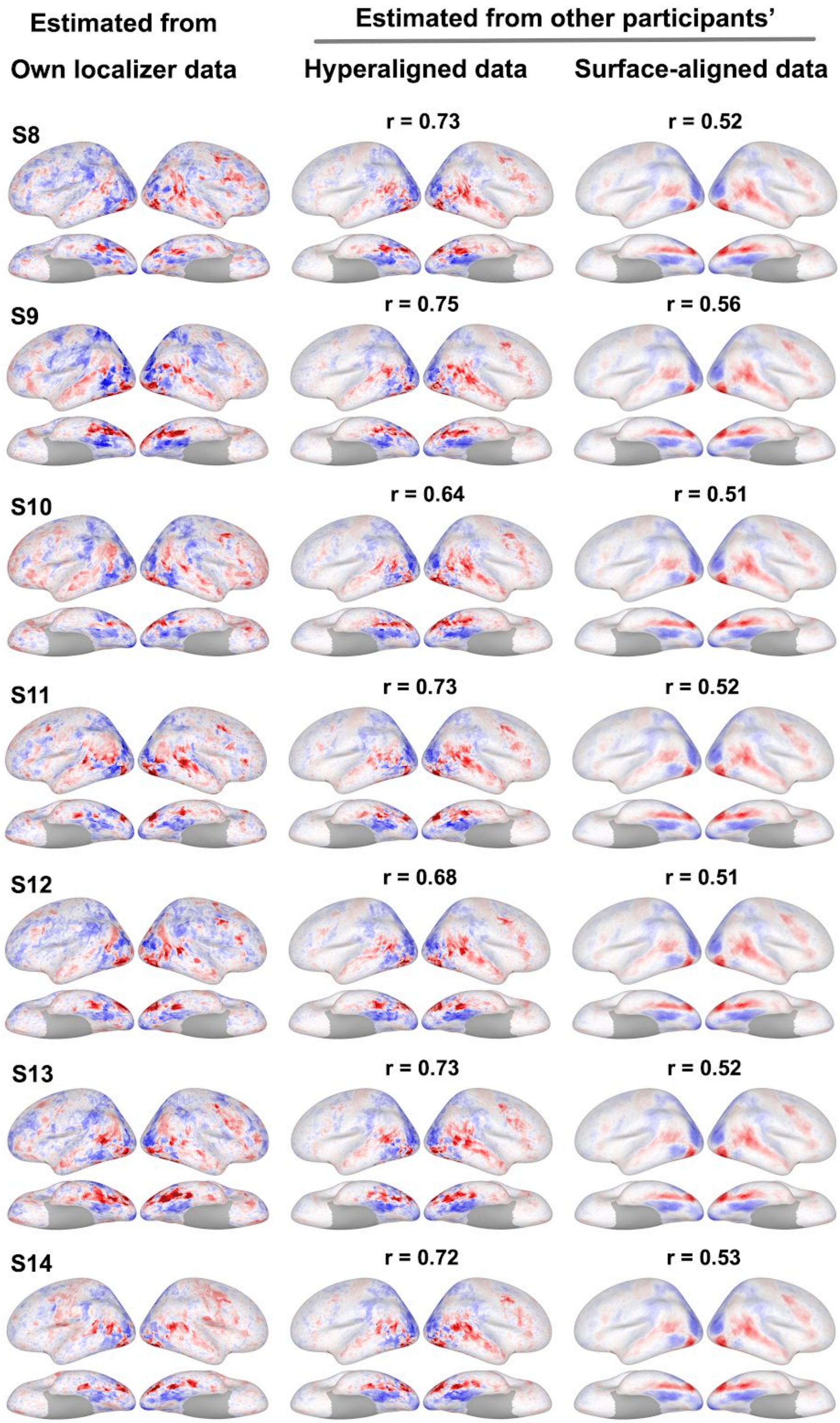
Estimated from
Own localizer data
Estimated from other participants'
Hyperaligned data
Surface-aligned data
S8
r = 0.73
r = 0.52
S9
r = 0.75
r = 0.56
S10
r = 0.64
r = 0.51
S11
r = 0.73
r = 0.52
S12
r = 0.68
r = 0.51
S13
r = 0.73
r = 0.52
S14
r = 0.72
r = 0.53

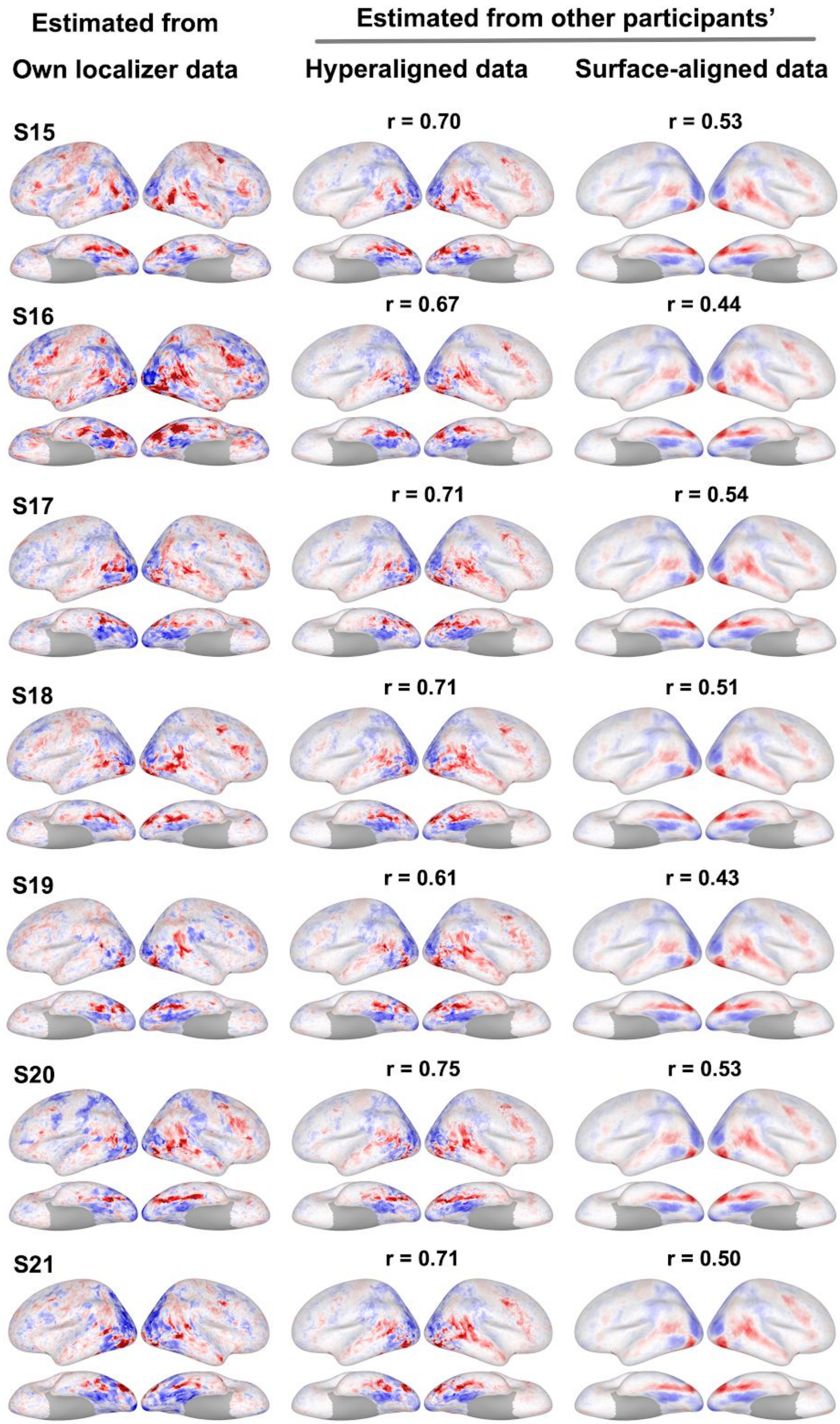

Estimated from
Own localizer data
Estimated from other participants'
Hyperaligned data
Surface-aligned data
S15
r = 0.70
r = 0.53
S16
r = 0.67
r = 0.44
S17
r = 0.71
r = 0.54
S18
r = 0.71
r = 0.51
S19
r = 0.61
r = 0.43
S20
r = 0.75
r = 0.53
S21
r = 0.71
r = 0.50

**Supplementary Figure 2. Contrast maps of individual participant (Grand Budapest dataset).** Contrast maps estimated from participants' own localizer data, the maps estimated from other participants' data with hyperalignment and with surface alignment were plotted for each participant in Grand Budapest dataset. The same with Supplementary Figure 1, correlation values above maps that were estimated from other participants' hyperaglined data indicate correlations between maps from participants' own data and the predicted maps with hyperalignment. Correlation values above maps that were estimated from other participants' surface-aligned data indicate correlations between maps from participants' own data and the predicted maps with surface alignment.

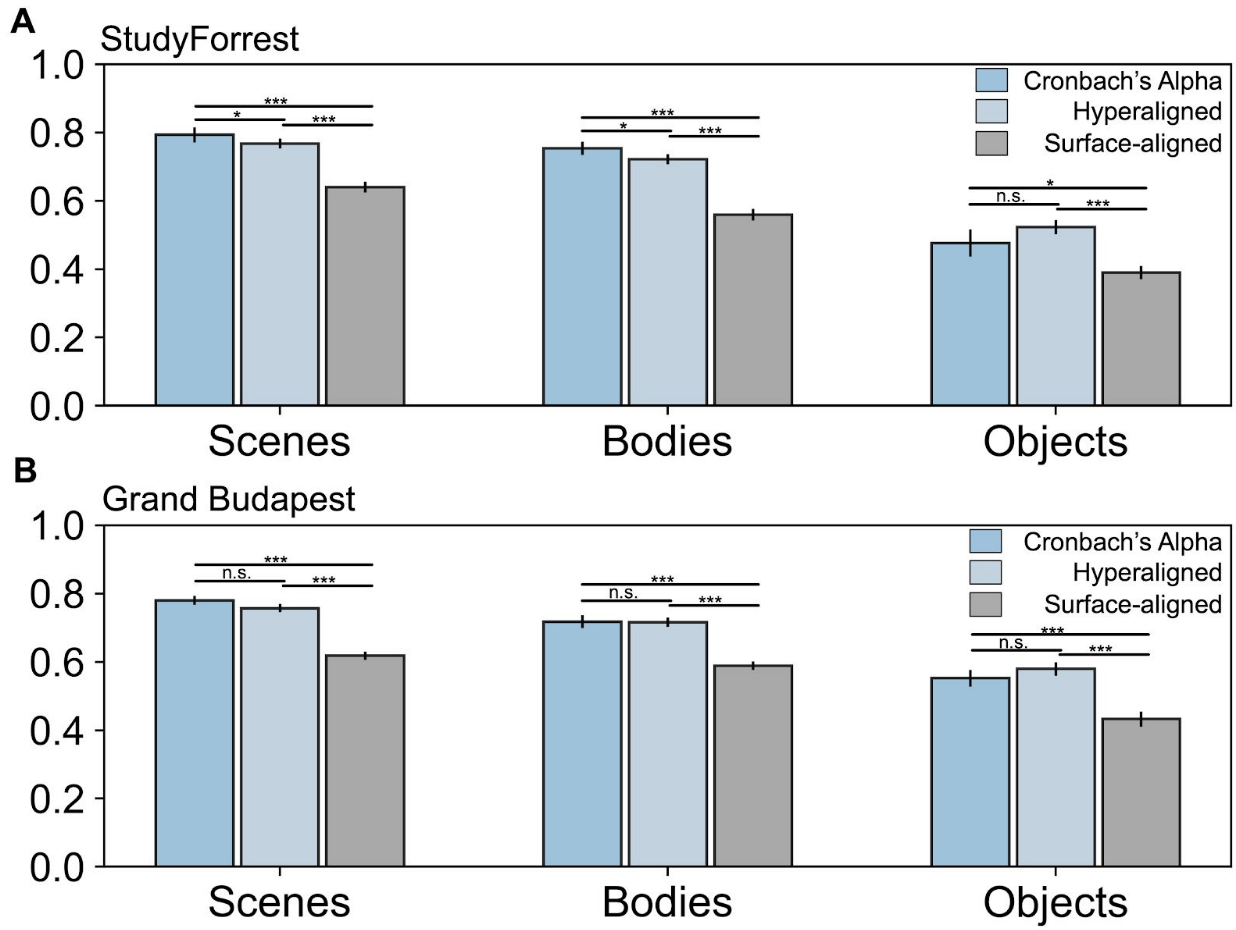


**Supplementary Figure 3. Predicting individual scene-, body-, and object-selective topographies.** We extended analyses following the procedures for estimating face-selective topographies to scene-, body-, and object-selective topographies using both the Grand Hotel Budapest and StudyForrest dataset. Scene-, body-, and object-selective topographies were defined with the contrast between responses to scenes (in the StudyForrest data set, both categories of scenes and houses were used in localizing scene-selective areas), bodies, objects, and the responses to all the other categories. Similar to face-selective topographies, category-selective topographies for scenes, bodies, and objects can be estimated with high-fidelity using hyperalignment. The correlation values between maps estimated from subjects' own localizer data and hyperaligned data are significantly higher than the correlations between maps estimated from their own localizer data and surface-aligned data (StudyForrest: Scene, $t(14) = 23.30$, $p < 0.001$; Body, $t(14) = 15.51$, $p < 0.001$; Object, $t(14) = 19.53$, $p < 0.001$.Grand Budapest: Scene, $t(20) = 29.30$, $p < 0.001$; Body, $t(20) = 36.01$, $p < 0.001$; Object, $t(20) = 19.67$, $p < 0.001$).

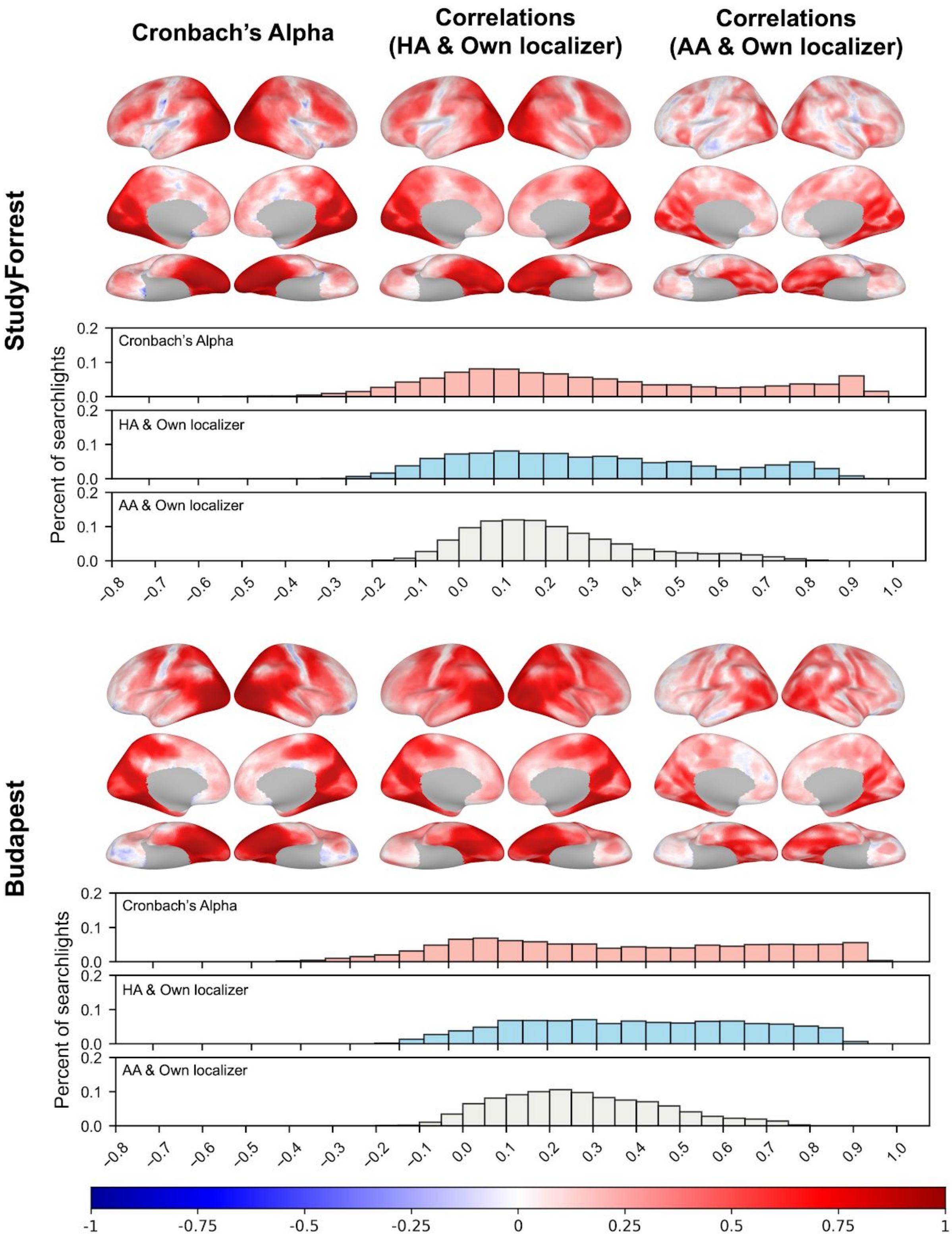


**Supplementary Figure 4. Searchlight analysis of Cronbach's alpha, correlations between scene-selective maps from participant's own localizer data and data estimated from others'**

**hyperaligned or surface-aligned data.** The upper two rows are results based with StudyForrest data set, and the bottom two rows are based on Grand Budapest data set. Within each data set, Cronbach's alpha of scene-selective maps cross four localizer runs (left), correlations between maps from participant's own localizer data and data estimated from others' hyperaligned (middle) or surface-aligned data (right) were calculated in each searchlight (15 mm radius) and plotted on the surface. Histogram plots with bin size of 0.05 are displayed for Conbach's alpha and those two maps accordingly. In searchlights that included strongly scene-selective cortical fields (e.g. occipital cortex, parahippocampal gyrus, retrosplenial cortex) correlations with estimates based on hyperaligned data exceeded 0.8.

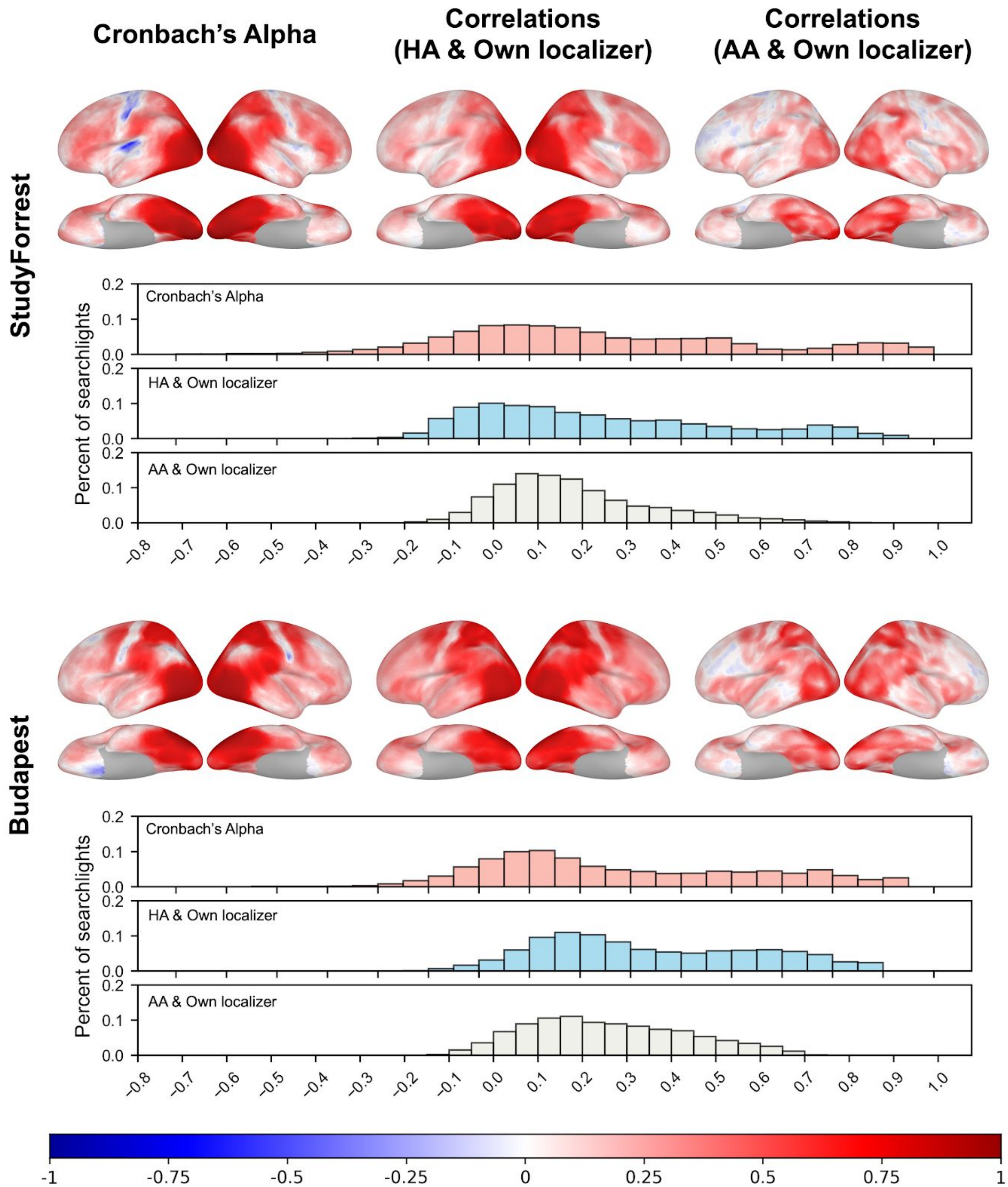


**Supplementary Figure 5. Searchlight analysis of Cronbach's alpha, correlations between body-selective maps from participant's own localizer data and data estimated from others' hyperaligned or surface-aligned data.** The upper two rows are results based with StudyForrest data set, and the bottom two rows are based on Grand Budapest data set. Within each data set, Cronbach's alpha of body-selective maps cross four localizer runs (left), correlations between maps from participant's own localizer data and data estimated from others' hyperaligned (middle) or surface-aligned data (right) were calculated in each searchlight (15 mm radius) and plotted on the surface. Histogram plots with bin size of 0.05 are displayed for Conbach's alpha and those two maps accordingly. In searchlights that included strongly body-selective cortical fields (e.g. ventral temporal cortex,  extrastriate visual cortex) correlations with estimates based on hyperaligned data exceeded 0.8.

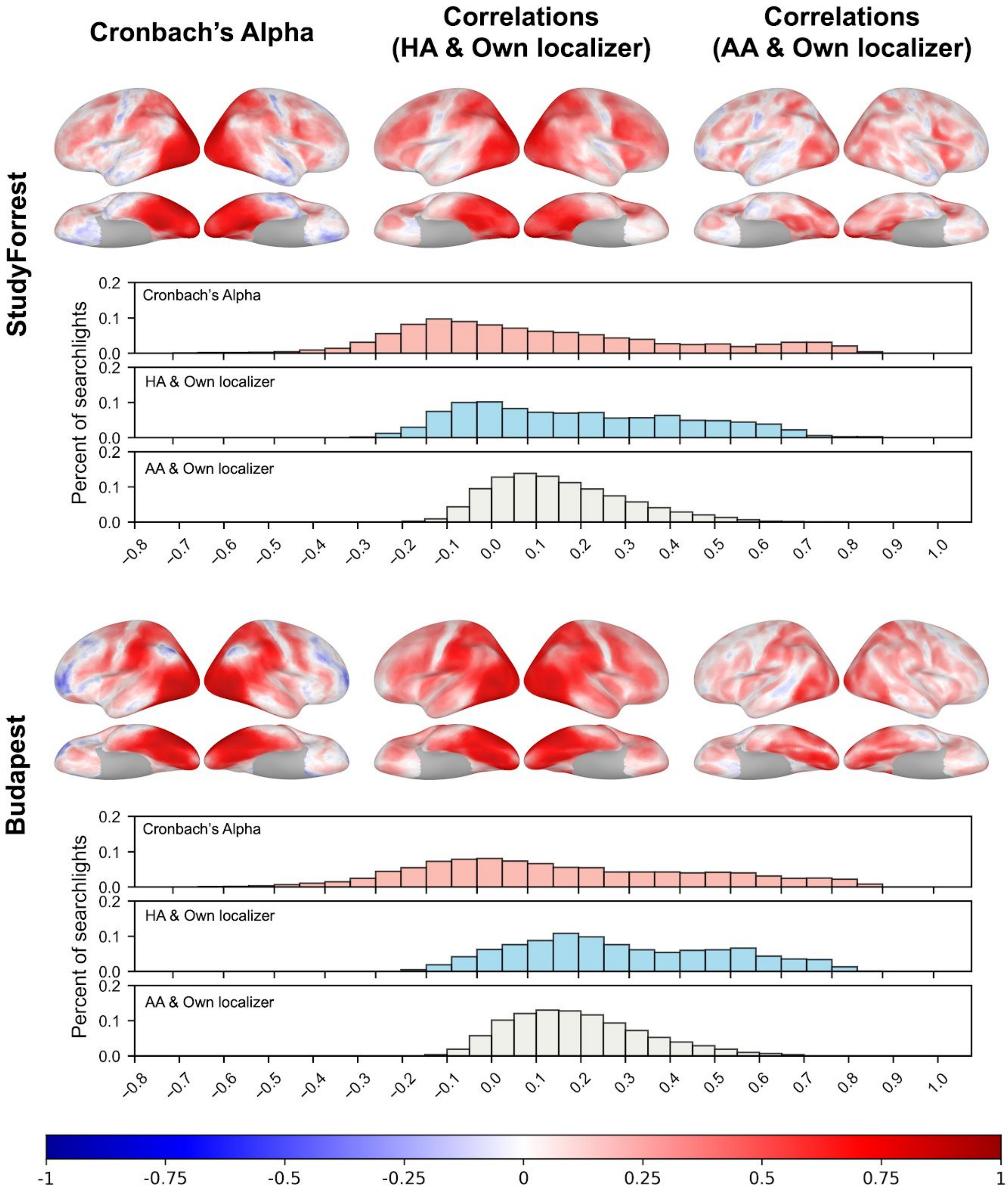


**Supplementary Figure 6. Searchlight analysis of Cronbach's alpha, correlations between object-selective maps from participant's own localizer data and data estimated from others' hyperaligned or surface-aligned data.** The upper two rows are results based with StudyForrest data set, and the bottom two rows are based on Grand Budapest data set. Within each data set, Cronbach's alpha of object-selective maps cross four localizer runs (left), correlations between maps from participant's own localizer data and data estimated from others' hyperaligned (middle) or surface-aligned data (right) were calculated in each searchlight (15 mm radius) and plotted on the surface. Histogram plots with bin size of 0.05 are displayed for Conbach's alpha and those two maps accordingly. In searchlights that included strongly object-selective cortical fields (e.g. ventral temporal cortex) correlations with estimates based on hyperaligned data exceeded 0.7.

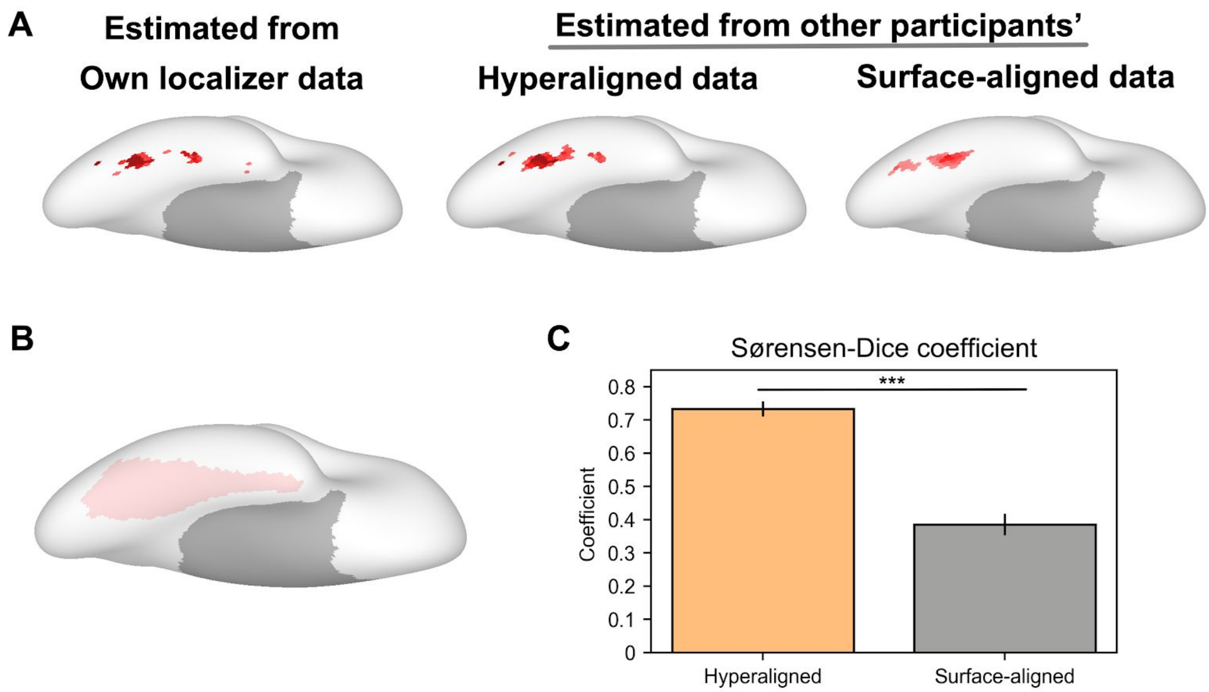


**Supplementary Figure S7. Identification of face-selective areas from topographic maps produced with hyperaligned data from other participants.** (A) The right FFA was estimated by selecting the top 10% face-selective vertices in an anatomical mask for the right fusiform gyrus (B) The right fusiform anatomical mask from the Freesurfer cortical parcellation Desikan-Killiany Atlas, (Desikan et al., 2006). (C) The Sørensen-Dice overlap coefficient. Over 70% of face-selective vertices were shared by the FFAs estimated from one's own localizer data and others' hyperaligned data, less than 40% of vertices were shared by FFAs estimated from own localizer data and others' surface-aligned data. The overlap for the FFA identified from hyperaligned data was significantly greater than that for surface-aligned data ($t(20) = 10.89$, $p < 0.001$), demonstrating that the maps from others' hyperaligned localizers can be used to identify individual category-selective areas.